Environmental Science and Pollution Research (2023) 30:65160–65176
https://doi.org/10.1007/s11356-023-26889-3

RESEARCH ARTICLE

Effectiveness and durability of anti-graffiti products applied on ETICS: towards a compatible and sustainable graffiti removal protocol

Bernardo Catita Gil[1] · Giovanni Borsoi[2,4] · João Luís Parracha[2,4] · Amélia Dionísio[3] · Rosário Veiga[4] · Inês Flores-Colen[2]

Received: 18 January 2023 / Accepted: 4 April 2023 / Published online: 20 April 2023

Abstract

External Thermal Insulation Composite Systems (ETICS) are widely used constructive solutions which aim at enhancing the building thermal performance. Nevertheless, ETICS can often present anomalies (e.g., stains and microcracks) throughout their service life, and vandalism actions, as in the case of graffiti, are rather common in urban areas. The removal of undesired graffiti is generally carried out through invasive chemical–mechanical methods, which may affect the durability of the ETICS. The adoption of anti-graffiti products can be a feasible protection method; however, no comprehensive studies were already addressed on these substrates. This study aims at evaluating the effectiveness, compatibility, and durability of three anti-graffiti products (with permanent, semi-permanent, and sacrificial properties) when applied on different ETICS. The removal of aerosol graffiti paints was carried out with a low-invasive and eco-friendly removal method (i.e., low-pressure steam jet). The water transport properties, as well as color, gloss, and roughness, were evaluated before and after graffiti removal. The durability of the anti-graffiti was also assessed by artificial aging cycles. Results showed that graffiti removal was rather efficient on ETICS with acrylic-based finishing coats and when using (semi) permanent anti-graffiti products (with $\Delta E^*_{ab} < 5$, i.e., not macroscopically visible, when comparing cleaned and reference surfaces), although these products can reduce their effectiveness after aging. Conversely, unsatisfactory graffiti cleaning was observed on ETICS with lime-based or silicate-based finishing coats (with $\Delta E^*_{ab} > 5$), with considerable alteration also of the water transport properties (reducing water absorption and slowing down the drying kinetic).

Keywords ETICS · Graffiti removal · Anti-graffiti products · Effectiveness · Compatibility · Durability

Introduction

The need to enhance the building energy efficiency and thus reduce greenhouse gas emissions led to the implementation of demanding national and international directives and regulations on the building environment (EU 2018). Therefore, sustainable constructive solutions, which can contribute to the hygrothermal performance and comfort of the building envelopes, have been adopted both in new construction and for the thermal retrofitting of building facades. External Thermal Insulation Composite Systems (ETICS), also known as EIFS (External Insulation Finishing Systems), are among the most commonly used solutions in the construction industry, due to their contribution to the building energy efficiency, as well as relatively low installation cost, mitigation of thermal bridges, and protection of the masonry and structural elements (Barreira and de Freitas 2014; Pasker 2017; Malanho and Veiga 2020). However, significant surface condensation might occur on the external surface of ETICS, due to its relevant thermal inertia, often favoring further esthetic anomalies (e.g., discoloration, formation of stains, and biological colonization). Runoff

Responsible Editor: George Z. Kyzas

✉ Giovanni Borsoi
giovanni.borsoi@tecnico.ulisboa.pt

[1] DECivil, Instituto Superior Técnico, University of Lisbon, Av. Rovisco Pais, 1049-001 Lisbon, Portugal

[2] CERIS, DECivil, Instituto Superior Técnico, University of Lisbon, Av. Rovisco Pais, 1049-001 Lisbon, Portugal

[3] CERENA, DER, Instituto Superior Técnico, University of Lisbon, Av. Rovisco Pais, 1049-001 Lisbon, Portugal

[4] Buildings Department, LNEC, National Laboratory for Civil Engineering, Av. Do Brasil, 101, 1700-066 Lisbon, Portugal

pollution, mainly caused by organic compounds (e.g., polycyclic aromatic or petroleum hydrocarbons), heavy metals, or other suspended particulate matter, can lead to the formation of carbon coatings on ETICS, affecting their physical and chromatic properties (Zhang et al. 2021). Thus, the constant exposure to weathering and anthropic agents may significantly affect the thermal efficiency and durability of these systems (Barreira and de Freitas 2014; Malanho and Veiga 2020).

Among the most common esthetic anomalies in urban environment, graffiti are frequently identified on ETICS (Amaro et al. 2014). It is worth noting that the proliferation of unauthorized tags and graffiti is often associated to urban decline and delinquency, and relevant financial resources have been spent in cleaning actions (Graffolution 2016).

Graffiti can be carried out using different products (e.g., paints, markers, pens, chalk, and waxy substances), although spray paints can be considered the most widely used material by graffiti-writers (Urquhart 1999). Aerosol spray paint are generally formulated with synthetic resin-based binders, i.e., alkyds, acrylics, and more rarely polyvinyl acetates, polyurethanes, or polyesters (Urquhart 1999; Sanmartín et al. 2014). Alkyd resins usually provide high durability and fast drying, whereas acrylics guarantee long-term esthetic stability and suitable flexibility (Urquhart 1999; Sanmartín et al. 2014).

The application of a new layer of paint on the graffiti is the most common intervention strategy; however, previous studies showed that the repetition of this action can alter the physicochemical properties of the original substrate, with shades and patches of different colors (Sanmartín et al. 2014; Feltes et al. 2023; Ribeiro et al. 2009). The application of graffiti, as well as its removal, can also induce an alteration of the water absorption and drying kinetics of the ETICS, with possible acceleration of the degradation processes (Feltes et al. 2023).

Graffiti removal is thus a necessary procedure, which intends to restore the esthetical properties of the surface and minimize possible physical–chemical effects of the graffiti paint on the substrate. Nevertheless, graffiti removal can be a difficult task, due to the high adherence of the aerosol spray paint to the tagged surface. Furthermore, widely used chemical–mechanical methodologies, e.g., acid or alkaline removers or high-pressure water jet (Feltes et al. 2023), can be inefficient and incompatible with composite systems, inducing lacunae and material and cohesion loss in the base and finishing coats of the ETICS and affecting the stability and durability of the substrate (Feltes et al. 2023).

A protection coating, which can facilitate graffiti removal and minimize possible detrimental effects or appearance of anomalies on the cleaned surface (Gomes et al. 2017; Elvira et al. 2013), can be provided by using anti-graffiti products, which were previously studied in several porous building materials, such as stone, mortars, and brick (Moura et al. 2014, 2017; García et al. 2010; Ricci et al. 2020; Lettieri and Masieri 2014; Carmona-Quiroga et al. 2010; Neto et al. 2016). In fact, these products could cover the surface or penetrate through the pore system of the treated substrate, forming a protective coating against the colorants, dyes, binder or additives of sprays, markers, and other materials used for graffiti (García and Malagab 2012).

Numerous anti-graffiti products, classified as sacrificial (i.e., allowing only one graffiti removal action, due to the elimination also of the anti-graffiti), semi-permanent (2 to 3 graffiti removal actions, without removing the product), or permanent (numerous graffiti removal cycles), are commercially available (Moura et al. 2014, 2017; García et al. 2010; Ricci et al. 2020). Anti-graffiti products are usually formulated with silica-based hybrid products or fluorinated compounds, and dispersed in water or organic solvent (Elvira et al. 2013; Moura et al. 2014; Carmona-Quiroga et al. 2008; Boostani and Modirrousta 2016). Products based on polysaccharides or nanocomposite materials can be also found in the market (Rabea et al. 2012; Masieri and Lettieri 2017).

These products generally present hydrophobic and oleophobic properties with high crosslinking density (Elvira et al. 2013; Lettieri et al. 2019), reducing the surface energy at the interface and thus minimizing the penetration of water, paints, and inks into the treated substrate. The formation of a hydrophobic barrier normally induces an alteration of the water vapor permeability of the substrate (Gomes et al. 2017; Carmona-Quiroga et al. 2008).

Although most of anti-graffiti can be considered chemically stable and solar radiation resistant (Rossi et al. 2016), the use of anti-graffiti products on stone, mortars, and brick showed in some cases that these products can be ineffective in the cleaning action and potentially harmful to the substrate (Gomes et al. 2017; Lettieri and Masieri 2014).

In this study, the effectiveness of graffiti removal on ETICS is evaluated through a fine-tuned methodology, which combine the use of anti-graffiti products and a sustainable removal method based on the use of a low pressure (3 bar) steam jet (Parracha et al. 2021a, b; Roncon et al. 2012). The compatibility of 3 anti-graffiti products was verified by evaluating some physical properties (roughness, color, and gloss) and the water transport (capillary absorption and drying) characteristics of ETICS. The durability of the anti-graffiti-coated ETICS to an accelerated aging procedure (i.e., hygrothermal cycles) was also assessed.

Materials and methods

Materials

ETICS

Four different commercially available ETICS systems, with different thermal insulation boards (expanded polystyrene—EPS; mineral wool—MW; expanded cork agglomerate—ICB), base coat (cementitious and/or natural hydraulic lime-based), and finishing coat (acrylic, silicate, or lime-based), were analyzed (Table 1). These systems have European Technical Approval (ETA), thus presenting suitable quality and adequate performance, following the EOTA requirements (EOTA 2019). Specimens with average dimensions of 15×15 cm^2 (used for the initial characterization of the specimens, prior to graffiti application) or of 15×7 cm^2 (used for the specimens with graffiti applied) and variable thickness (Table 1) were used and stored at controlled laboratorial conditions (T = 20 °C, RH = 65%) for several days prior to testing.

Moreover, specimens were sealed on the lateral side with adhesive metallic tape to protect the cross section and avoid lateral diffusion flow (towards the base coat and thermal insulation) during graffiti application and removal.

The thermal conductivity coefficient (λ) of the considered ETICS ranges from 0.037 W/(m·K) in the case of the EPS-based systems, 0.045–0.047 W/(m·K) in the case of the ICB-based systems, and 0.040–0.041 W/(m·K) in the case of the MW-based systems (Parracha et al. 2021a). Regarding the basecoat, the density of the varies from 1.3–1.6 g/cm^3 in the case of the cementitious formulations, to 1.2–1.35 g/cm^3 in the case of lime-based formulations (with light cork-based aggregate). Furthermore, the different acrylic-based coatings presented a slightly higher density (1.5–1.8 g/cm^3), if compared to the silicate-based coatings (1.4 g/cm^3).

Graffiti aerosol paints

Two aerosol graffiti paints, i.e., ultramarine blue (RAL code RV-5002), identified as B, and silver-gray (RAL 7001), identified as S, from Montana Colours TM S.L, were selected, based also on previous studies (Pozo-Antonio et al. 2018; Rivas et al. 2012). These aerosol paints are formulated with a polymeric binder (alkyd nitrocellulose resin for blue paint; polyethylene resin for silver paint) with different fillers and/or charges (Germinario et al. 2016). The ultramarine blue paint contains also TiO_2 (14.2% in mass) and SiO_2 (5%), whereas oxides and salts are used as blue chromophores. The silver-gray paint is formulated with significant addition of Al_2O_3 (19.4%) (Fiorucci et al. 2011).

A consumption per application of 0.022 ± 0.009 g/cm^2 and 0.032 ± 0.011 g/cm^2 were registered for the blue and silver paints, respectively. The high standard deviation values are related to the higher amount of paint retained in the specimens with slightly more porous or rough finishing coats. Applications were carried out on three replica specimens of every type of systems.

Anti-graffiti products

Three commercial anti-graffiti products, with different properties (i.e., sacrificial, semi-permanent, permanent), were tested (Table 2). The anti-graffiti product identified as AG1 is based on an acrylic-based aqueous solution, containing also waxes, ethoxylated alcohols, and biocides; the product AG2 is a nanostructured aqueous solution based on silicon oxide and titanium, containing also biocidal additives; the anti-graffiti product AG3 is a solution of polyorganosiloxane dispersed in organic solvents (hydrocarbons, ethanol, alkanes), with biocides.

Table 1 Characteristics of the components of ETICS (based on the product data sheets) (EPS—expanded polystyrene; ICB—expanded cork agglomerate; MW—mineral wool board). *Includes a reinforced glass fiber mesh

System (S)	Thermal insulation (TI)	Base coat (BC)*	Finishing coat (FC)		Thickness (mm)
			Key-coat	Finishing	
S1	EPS	Cement, synthetic resins, mineral additives	Water-based acrylic dispersion	Water-based acrylic co-polymer, pigments, marble powder, and additives	≈42
S2	ICB	Natural hydraulic lime, cement, mineral fillers, resins, and synthetic fibers	Air lime, hydraulic binder, and organic additives		≈65
S3	MW	Cement, synthetic resins, mineral fillers, and additives	Water-based acrylic co-polymer and mineral additives	Water-based acrylic paint, mineral aggregates, pigments, and additives	≈42
S4	ICB	Natural hydraulic lime, cement, mixed binders, and cork aggregates	Water-based dispersion of silicate	Water-based silicate paint, organic additives, and pigments	≈65

Table 2 Properties of the anti-graffiti products (based on technical and safety data sheets)

Identification	Anti-graffiti product type	Color	Density (g/ml) at T = 20 °C	Consumption (l/m^2)	pH	Flash point
AG1	Sacrificial	Whitish, light yellow	1.01 ± 0.04	0.08–0.12	8.5 ± 0.5	> 67 °C
AG2	Semi-permanent	Whitish, light gray	1.00 ± 0.02	0.04–0.12	11.0 ± 0.5	> 60 °C
AG3	Permanent	Light yellow	0.98 ± 0.01	0.11–0.14	9.0 ± 0.5	55 °C

Graffiti application and removal

Anti-graffiti products were applied by brushing with no dilution and at ambient temperature (T ≈ 20 °C) (Fig. 1a), applying two coats in orthogonal directions and with a 24-h interval. An amount of product between 0.02 (in the case of S4, considerably less rough and compact) and 0.05 l/m^2 (with S2 and S3, noticeably rougher and possibly more absorbent) was applied for each coat, i.e., the amount necessary to completely cover the treated surface.

Afterwards, the aerosol paints B and S were applied on specimens with and without anti-graffiti products using spray cans at a 45° angle and at 15 cm from the surface (Fig. 1b), in accordance with ASTM D7089 (ASTM 2014). From the standard, it was established that an application by spraying in threefold during 1 s, in two distinct directions, was suitable to homogeneously cover the surface of the specimens. After these applications, the specimens were stored in a conditioned room (T = 20 °C, RH = 50%) for 15 days, in order to facilitate a complete polymerization of the aerosol paints (Careddua and Akkoyunb 2016).

The graffiti paints were then removed using a steam washer (Karcher SC1) at low pressure (3 bar) (Fig. 1c), by combining the steam jet with manual brushing. The brushing action was repeated in orthogonal directions, repeating the procedure up to 6 times in some cases, depending on the level of cleaning achieved. This method, which was selected based also on previous works (Feltes et al. 2023), might provide, if associated to the use of anti-graffiti products, a proper graffiti removal with minimization of detrimental effects on the cleaned surface.

Methods

The physical surface features (color, gloss, roughness) and the water transport properties of the ETICS at different phases (i.e., pristine, after anti-graffiti application, after graffiti paint removal) were evaluated in order to verify the compatibility of the anti-graffiti products when applied on ETICS specimens, as well as the effectiveness of the anti-graffiti products in the graffiti removal. Additionally, the durability of the specimens with and without anti-graffiti products to hygrothermal cycles was assessed, as described below.

Surface roughness

The surface roughness was evaluated using an Elcometer 223 surface profile gauge (peak-to-valley measurement), with a 0.001-mm resolution. A surface grid was used on the surface of the specimens in order to allow the repetition of the measurements in the same points, considering the average value of 6 measurements per specimen and relative standard deviation.

Esthetic properties

The specular gloss was measured according to ASTM D6578 (ASTM 2018), using a PCE-PGM 100 (incidence angle of 60°; measurement range 0–1000 GU—gloss units, resolution 0.1 GU). A surface grid was used, analyzing 6 measurements per specimen and considering the average values and relative standard deviation.

A Minolta CR-410 portable colorimeter was used to measure the colorimetric coordinates, considering the CIELAB color space (L^*—lightness; a^*—red/green coordinates; b^*—yellow/blue coordinates) and adopting the ASTM D2244 standard (ASTM 2016). The measurements were conducted in specular component included mode (SCI), applying a standard illuminant D65 and a

Fig. 1 **a** Application of anti-graffiti products; **b** application of aerosol paints (ultramarine blue); **c** removal of graffiti with a low-pressure steam jet and brushing

Table 3 Details of the hygrothermal cycles

Heat-rain cycles	Heat-cold cycles
Heating infrared lamps (3 h, T = 70 ± 5 °C, RH = 10/30%) Sprinklers (1 h, 1 l/(m^2·min) of sprayed water, T = 15 ± 5 °C)	Heating infrared lamps (8 h, T = 50 ± 5 °C, RH < 30%) Deep freeze (16 h, T = − 20 ± 5 °C)

measurement angle of 2°, in an approximate area of 50 mm^2. The total color variation (ΔE^*_{ab}) between different phases of the study was calculated according to that recommended in ASTM D2244 (ASTM 2016), according to Eq. 1:

$$\Delta E^*_{ab} = \sqrt{(\Delta L^*)^2 + (\Delta a^*)^2 + (\Delta b^*)^2} \quad (1)$$

where ΔE^*_{ab} is the color variation between two consecutive phases of the study; ΔL^*, Δa^*, and Δb^* the variations in luminosity (L^*) and the colorimetric coordinates a^* and b^*, respectively. Saturation (chroma—C^*_{ab}), which represents the degree of purity of the relative color in comparison to neutral gray ($C_{ab} = 0$), was also determined according to (CIE 2014), using Eq. 2:

$$C^*_{ab} = \sqrt{(a^*)^2 + (b^*)^2} \quad (2)$$

The efficacy of the graffiti removal was assessed evaluating the residual stain (*RS*) after cleaning (%) (Masieri and Lettieri 2017), in accordance with Eq. 3:

$$RS = \frac{(\Delta E^*_{ab})_c}{(\Delta E^*_{ab})_s} * 100 \quad (3)$$

where $(\Delta E^*_{ab})_c$ is the color variation of the cleaned surfaces and $(\Delta E^*_{ab})_s$ is the color variation of the stained surfaces.

Water transport properties

The capillary water absorption test was carried out based on the procedure defined by EAD 040,083–00-0404 (EOTA 2019) in a conditioned room (T = 23 ± 2 °C; RH = 65 ± 5%). The finishing coat of the specimens was partially immersed in water (2–3 mm water depth), monitoring the amount of water absorbed at specific intervals (3 min, 1 h, 2 h, 4 h, 8 h, and 24 h).

The capillary water absorption curves were plotted and the capillarity coefficient was determined considering the slope of the initial phase of the capillary absorption curve, based on a linear regression (interval 0–3 min) (Parracha et al. 2021a; Roncon et al. 2012), according to Eq. 4:

$$C_c = \frac{M_1 - M_2}{A\sqrt{0.05}} \quad (4)$$

where C_c is the coefficient of water absorption by capillarity (kg/m^2·h$^{0.5}$); M_1 the initial sample mass (kg); M_2 the sample mass (kg) after 3 min of absorption; A the sample area (m^2).

The drying kinetics was evaluated according to EN 16,322 (CEN 2013). After the capillary water absorption test, specimens were stored in a conditioned room (T = 23 ± 2 °C, RH = 65 ± 5%) and weighted at given time intervals (10, 30 min; 1, 2, 4, 8, 24, 48, 72, 144, and 168 h) until mass stabilization (mass variation < 1% between two consecutive measurements). The drying rates were calculated in phase 1

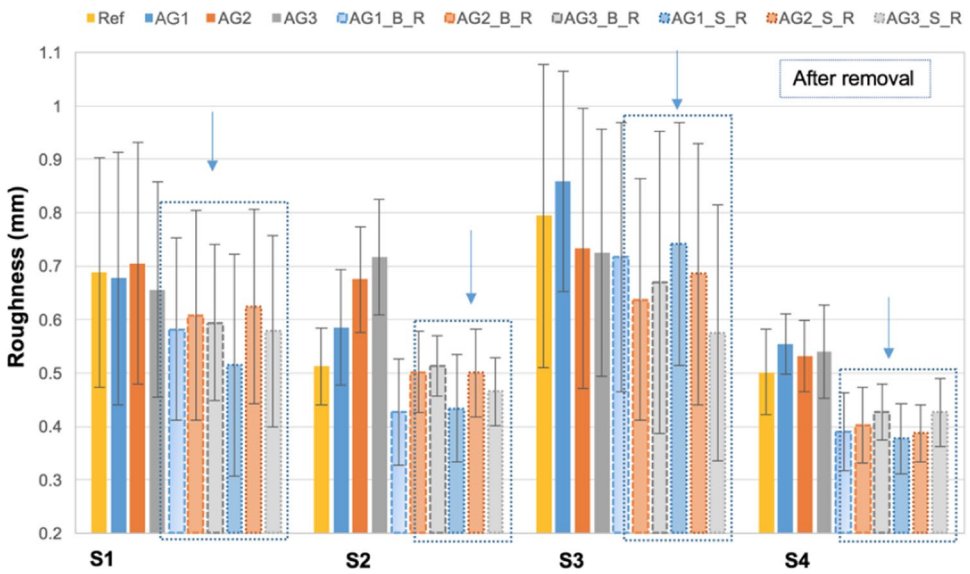

Fig. 2 Surface roughness and relative standard deviation of reference specimens (Ref), after application of anti-graffiti products (AG1, AG2, AG3), and after graffiti removal (B = blue paint; S = silver paint; R = after graffiti removal)

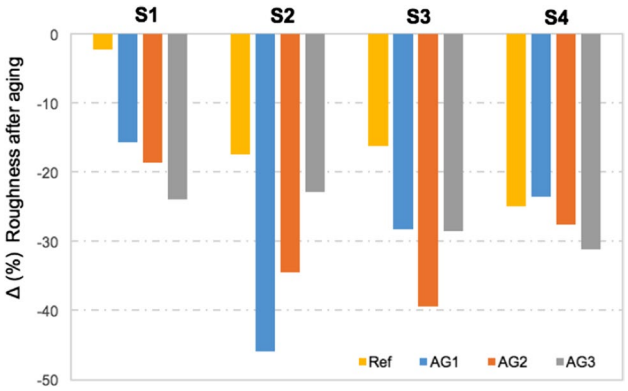

Fig. 3 Variation of surface roughness after artificial aging of the reference specimens (Ref) and of the specimens with anti-graffiti products (AG1, AG2, AG3)

(TS1, in the liquid phase) and in phase 2 (TS2, in the vapor phase), according to EN 16,322 (CEN 2013).

Accelerated aging test

The durability of the specimens was assessed through accelerated aging tests with hygrothermal cycles (heat-rain and heat-cold cycles), in accordance with EAD 040,083–00-0404 (EOTA 2019) (Table 3).

The hygrothermal cycles were carried out in a FitoClima 700EDTU climatic chamber from Aralab. The specimens were fixed on a rack at 50 cm from the sprinklers or from thermal IR lamps. Eighty heat-rain cycles were then performed (a total of 320 h), followed by five heat-cold cycles, in a total of 120 h (Table 3). Between the heat-rain and the heat-cold cycles, ETICS specimens were left to drain for 2 h and then conditioned at room temperature (15 °C ≤ T ≤ 25 °C; RH ≥ 50%) for 48 h.

Results

Surface roughness

The values of the surface roughness of the specimens at different test stages (i.e., references, after application of anti-graffiti products, and after graffiti removal) are shown in Fig. 2. Results indicate that the S3 system is the roughest (0.794 ± 0.324 mm), while the S4 system is the smoothest (0.502 ± 0.081 mm). As specified in previous studies (Gaspar et al. 2003; Carvalhão and Dionísio 2014), roughness variation is considered significant only when the difference between mean values is higher than the standard deviation determined for the reference ETICS, as can be seen in specimen S3 (rather rough and heterogeneous) (Fig. 2). After the application of the anti-graffiti products, the roughness slightly changed (≤ 10%) in the systems with acrylic-based or silicate-based finishing coat (S1, S3, and S4), and moderately increased in the case of system S2 (up to 40%), with a lime-based finishing coat and thus more absorbent surface.

The application of the graffiti paints generally induced a homogenization of the roughness in the specimens, with the paints filling the valleys of the surface (Ribeiro et al. 2009; Gomes et al. 2018). However, a smoothing was noticed after graffiti removal, especially in specimens S2 and S4 (natural hydraulic lime and silicate-based finishing, respectively). The moderate erosion and leaching of the materials, which constitute the base and finishing coats, can be attributed to the manual brushing of the surface.

After artificial aging, it can be observed a surface roughness reduction (15–25%) in the case of reference specimens S2 (lime-based finished), S3 (rough and acrylic-based finishing coat), and S4 (silica-based painted) (Fig. 3). The roughness of specimen S1 was almost unvaried; however, blistering and microcracks were observed on this aged specimen.

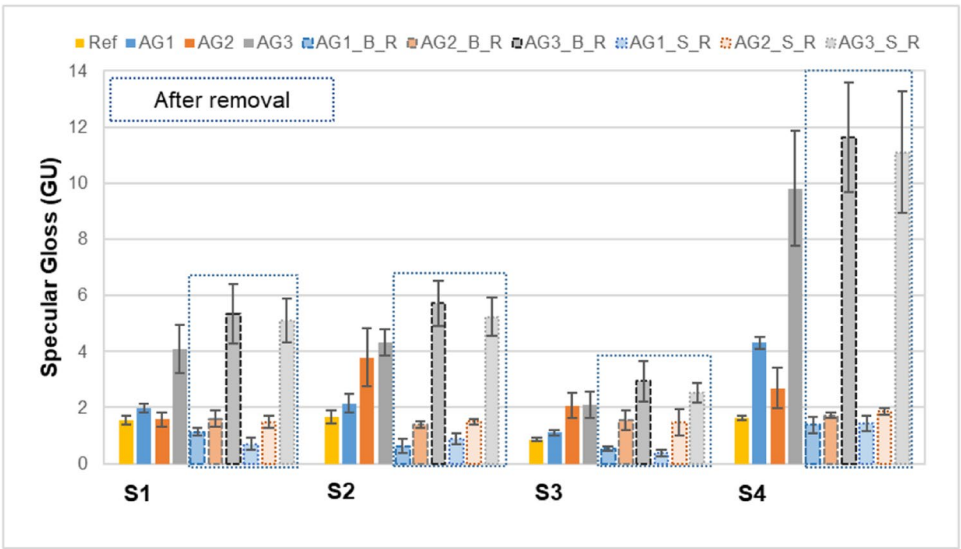

Fig. 4 Specular gloss and relative standard deviation of reference specimens (Ref), after application of anti-graffiti products (AGx), and after graffiti removal (B = blue paint; S = silver paint; R = after graffiti removal)

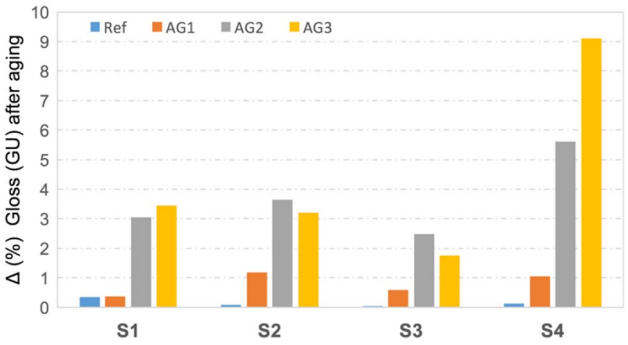

Fig. 5 Gloss variation after artificial aging of the reference specimens (Ref) and of the specimens with anti-graffiti products (AG1, AG2, AG3)

The hygrothermal cycles significantly reduced the surface roughness of the anti-graffiti products when applied on specimens S1 and S3 (up to 40%, with AG2 on S3), as well on S2 (lime-based finished, up to 45% with AG1), whereas no significant difference was observed among the specimens S4 with or without anti-graffiti products (reduction around 25–30% in all cases). Thus, the roughness of the anti-graffiti products applied on the systems with acrylic-based or lime-based finishing coat were more affected by repeated cycles of heat-rain and heat-cold.

Specular gloss

Systems S2 and S4 presented the highest values of specular gloss (1.64/1.66 GU, Fig. 4), being also the smoothest. Significantly lower values were observed in the case of S3 (0.86 GU) (Fig. 4). The application of the silver graffiti induced a considerably higher gloss, if compared to the blue graffiti, due both to the higher brightness properties of its polyethylene-based binder and alumina additives. After the application of the anti-graffiti products, it was observed that product AG3 (permanent) induced a remarkable gloss increase (around × 2/2.5 times in the case of specimens S1, S2, and S3, up to × 5 in the case of specimen S4). Furthermore, the application of the silver aerosol paint led also to a significant gloss variation (up to + 64%, in the case of S4.AG3.S).

The removal of the graffiti paints was generally followed by a gloss decrease, with the most noticeable reduction obtained in the case of specimens with AG1. Conversely, the semi-permanent product AG2 maintained similar gloss values after removal, except for specimen S2 (with lime-based finishing). Finally, the AG3 product maintained high gloss values, with variations > 2 GU and therefore macroscopically visible (Parracha et al. 2021b), and the highest variation was observed in the case of specimen S4.AG3.B (10%). Therefore, sacrificial anti-graffiti product AG3, with slightly thicker coating and intense yellowish tone, affected more significantly the gloss of the ETICS surfaces (Fig. 4).

After artificial aging, it can be observed that the reference specimens were not affected, similarly to the specimens with AG1 (up to 1% increase in all systems), which was almost completely removed with the graffiti (Fig. 5). In the case of anti-graffiti products AG2 and AG3, a slight gloss increase was observed, with the highest values in the case of system S4. However, with exception of the products applied on system S4 (with silicate-based finishing coat), it can be concluded that artificial aging only moderately affected the surface gloss of the acrylic-based AG2 and siloxane-based AG3 anti-graffiti (semi) permanent products.

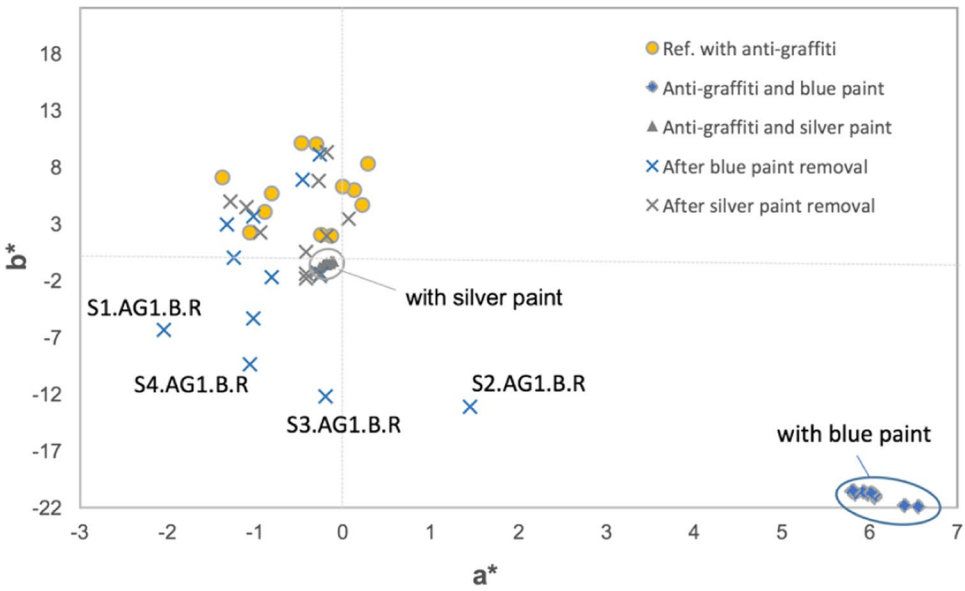

Fig. 6 Variation of CIELAB chromaticity coordinates *a** and *b** of the reference specimens after application of the anti-graffiti products (AGx) and after removal of graffiti (B = blue paint; S = silver paint; R = after graffiti removal)

Table 4 Color variation among pristine specimens and those after graffiti removal (in green $\Delta E^*_{ab} < 5$, in yellow $5 < \Delta E^*_{ab} < 10$, in red $\Delta E^*_{ab} > 10$ CIELAB units)

ETICS Systems	Without graffiti applied			After Blue Paint removal			After Silver Paint removal		
	AG1	AG2	AG3	AG1	AG2	AG3	AG1	AG2	AG3
S1	2.06	2.30	2.33	12.31	5.31	1.74	33.02	10.60	4.20
S2	3.54	1.54	6.01	40.95	8.56	6.17	33.20	6.85	6.69
S3	1.30	2.70	3.19	28.77	9.64	2.13	31.82	15.70	3.11
S4	1.24	1.93	4.10	16.32	9.20	3.15	31.62	5.77	4.06

Color

Results show that the reference specimens are close to an almost ideal white, with specimen S4 (with silicate-based finishing) presenting the highest luminosity ($L^* = 95.30$) and lowest chroma ($C^*_{ab} = 0.85$). The application of the anti-graffiti products induced a slight increase in the b^* chromatic coordinate, i.e., some specimens gained a yellowish tone, which is rather pronounced with AG1 and AG3. The application of the blue and silver paints led to an expectable, strong color change in all specimens ($\Delta E^*_{ab} \geq 61$ CIELAB units) (Fig. 6). It is worth noting that the metallic silver paint had luminosity and chroma values close to zero (Fig. 6), due to its high gloss (Fig. 4), attributed to the inclusion of aluminum particles.

The removal of the blue graffiti paint was not effective in the specimens with the sacrificial product AG1, maintaining a consistent blue tone after the cleaning process (negative b^* values) (Fig. 6). In fact, a suprathreshold color-difference was reached ($\Delta E^*_{ab} > 10$ CIELAB units) in the specimens with AG1, being significantly high in the case of the silver paint (Table 4) (Sanmartín and Pozo-Antonio 2020). Consequently, AG1 product is not effective in the removal of aerosol graffiti paints applied on ETICS, regardless of the type of ETICS system considered (Fig. 7a).

Conversely, the product AG3 led to an effective removal of the aerosol paint graffiti, with $\Delta E^*_{ab} < 5$ CIELAB units (i.e., below the ASTM standard limit (ASTM 2018), thus not macroscopically visible) after the removal of both paints (blue and silver), except for system S2 (lime-based finish). Finally, specimens with AG2 showed a reasonable efficiency in the removal of the blue paint, although some macroscopically visible shadows were visible at naked eye (Fig. 7b). Acceptable values were observed mainly in the smoother and acrylic-based finishing (as in the case of S1), and reasonable values in the case of the lime-based (S2) and silicate (S4) finishing (Fig. 7c). Thus, (semi) permanent anti-graffiti products AG2 and AG3 were rather effective in the removal of the tested aerosol paints.

It is worth noting that the silver paint was more difficult to remove, if compared to the blue paint; these values can be attributed to the formulation of the silver paint, composed also by a relevant amount of inert additives (aluminum oxide particles), which can hinder the mechanical removal (Figs. 5, 7d).

If comparing the previous values (Table 4) with the residual stain (*RS*) after cleaning (%), results showed that a similar trend can be observed after blue paint removal (Table 5), with feasible removal with product AG3 and unsatisfactory results with AG1. In fact, *RS* values below 10% can be considered suitable, among 10 to 20% not optimal but tolerable, and above 20% ineffective (Masieri and Lettieri 2017). Conversely, the *RS* values after silver removal were much higher if compared to the color variation values. These latter results were possibly affected by the high gloss and brightness of the silver graffiti, attributed to the inclusion of aluminum particles.

Table 5 Residual stain (*RS*) after blue and silver graffiti removal (%) (in green $RS < 10\%$, in yellow $10\% < RS < 20\%$, in red $RS > 20\%$)

ETICS Systems	RS					
	Blue Paint removal			Silver Paint removal		
	AG1	AG2	AG3	AG1	AG2	AG3
S1	18.51	7.93	2.66	> 400	> 80	> 50
S2	62.65	13.12	9.51			
S3	44.5	15.56	3.44			
S4	24.34	13.71	4.72			

Table 6 Color change among pristine specimens and those after artificial aging (in green $\Delta E^*_{ab} < 5$, in yellow $5 < \Delta E^*_{ab} < 10$, in red $\Delta E^*_{ab} > 10$ CIELAB units)

ETICS	Reference	Anti-graffiti products		
		AG1	AG2	AG3
S1	1.23	8.22	4.25	6.09
S2	6.02	13.59	7.40	13.55
S3	6.55	7.02	6.38	6.43
S4	1.44	8.39	3.66	7.39

When evaluating the chromatic coordinates of the specimens after artificial aging (Table 6), it can be observed that the reference specimens S1 and S4 were rather stable (Fig. 8a), whereas an increase of the b^* coordinate (i.e., yellowish/brownish color) was observed with systems S2 and S3 (Fig. 8b). Concerning the anti-graffiti products, AG2 showed the highest stability, i.e., the lowest color variation (values similar to the reference specimens) and thus chromatic durability, whereas AG1 and AG3 showed a significant color variation (yellowish tone), which is visible at naked eye.

Water absorption by capillarity

When comparing the reference specimens, system S1 (with an acrylic-based finishing coat) presented the lowest capillarity coefficient (0.035 kg/m^2·min$^{0.5}$), whereas system S2 (lime-based rendering system) obtained the highest C_c (0.122 kg/m^2·min$^{0.5}$) (Fig. 9), in agreement with previous studies (Parracha et al. 2021a, b; Roncon et al. 2012).

The application of the products AG2 and AG3 provided noticeable water-repellent properties to the ETICS surface. In fact, a decrease in the capillarity coefficient was registered in all systems, when compared to the reference specimens, especially in the case of S2.AG2 (−92%) and S2.AG3 (−90%). Conversely, a significant increase in the C_c (between 18 and 99%) was observed in the specimens with the product AG1, with exception of system S1. These results may be related to the presence of polysaccharides with hydrophilic properties (Lubelli et al. 2008) in the product AG1.

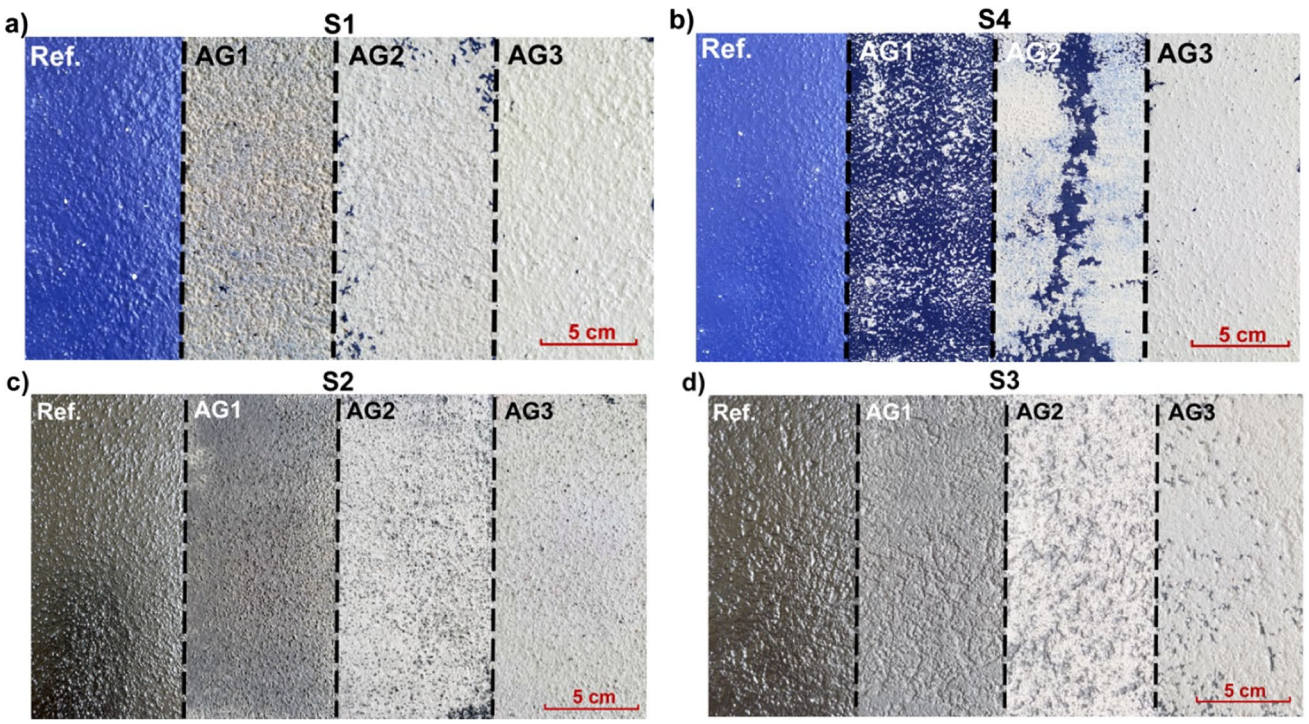

Fig. 7 Pictures of the specimens prior (Ref) and after graffiti removal, with the different anti-graffiti products (AG1, AG2, AG3): **a** S1 and **b** S4 with blue graffiti paint; **c** S2 and **d** S3 with silver graffiti paint

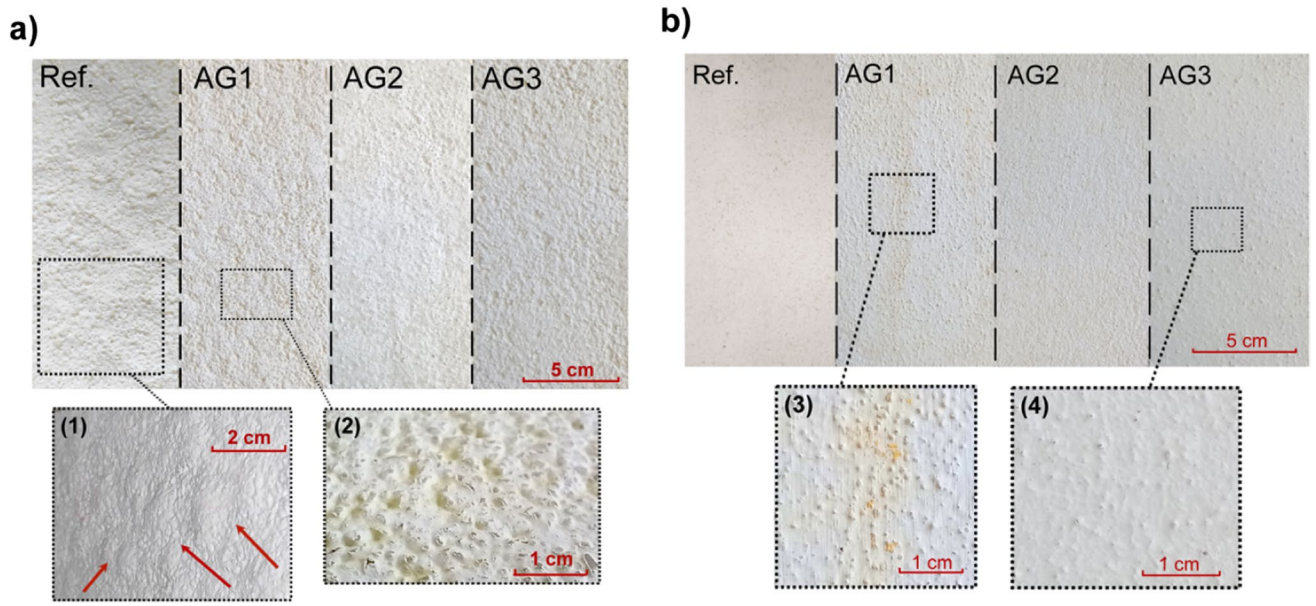

Fig. 8 Pictures of the specimens prior (Ref) and after artificial aging, with the different anti-graffiti products (AG1, AG2, AG3): **a** S1, where blistering (1) and a yellowish tone with microcracks (2) can be observed on the reference specimen and on that with AG1; **b** S2, where a yellowish/brownish pigment (3), attributed to the leaching of cork from the insulation board, and an homogenous and glossy (4) can be observed on the specimens with AG1 and AG3, respectively

The application of the (blue and silver) polymer-based, hydrophobic spray paints generally induced a C_c decrease, ranging from reduced (− 12% in the specimen S3.AG1.S) to significant (− 95% in the specimen S2.AG2.B) variations. After graffiti removal, the C_c values generally decreased, if compared to the initial state (Fig. 9), mostly in the case of specimen S2 (lime-based finishing render) and with the products AG2 and AG3 (3 to 6 times more hydrophobic than the reference specimen). The latter results can be attributed to the (semi-) permanent properties of these anti-graffiti products, which have protective and water-repellent properties. Conversely, the specimens with (sacrificial) product AG1 presented slightly higher C_c, due to its hydrophilic properties, as well as partial removal during the graffiti cleaning action and reduced removal efficiency (Fig. 7).

After aging, systems S2, S3, and S4 underwent a remarkable C_c decrease, possibly due to the run-off of the surface (Table 7). Dissolution–recrystallization processes of the cement or lime-based finishing coat might lead to a modification of the pore size distribution and consequent reduction of micro and capillary pores.

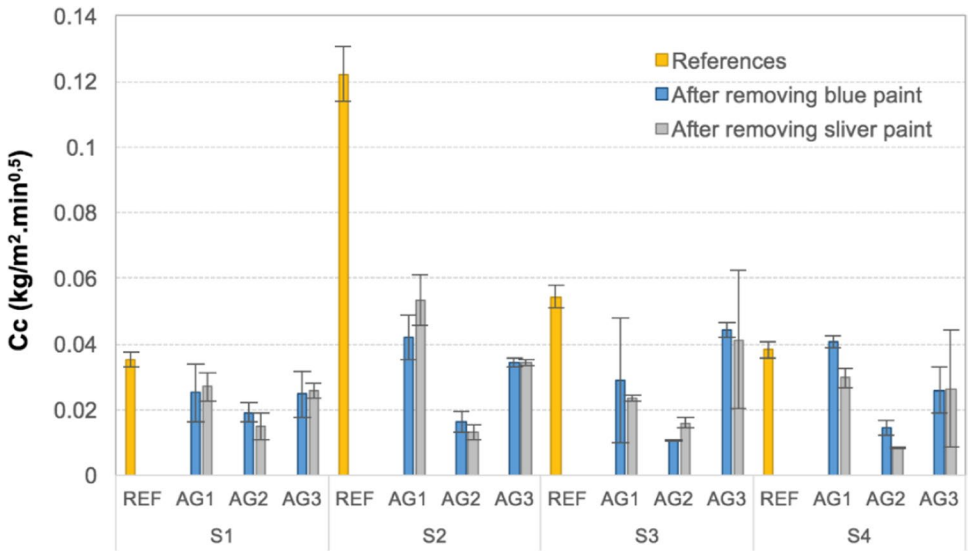

Fig. 9 Capillarity coefficients (C_c) and relative standard deviations of the reference specimens and after removal of the blue and silver paints

Table 7 Variation of the capillary absorption coefficient (C_c) (%) among pristine specimens and those after artificial aging (in green relevant increase ≥ 15%, in yellow: − 15% ≤ acceptable variation ≤ 15%, in red: significant decrease ≤ − 15%)

ETICS	Reference	Anti-graffiti products		
		AG1	AG2	AG3
S1	12.67	31.53	-0.15	38.90
S2	-48.39	-94.72	-0.19	-55.09
S3	-52.83	-31.40	9.59	59.87
S4	-59.13	-9456	-70.93	-66.68

Conversely, a C_c increase was observed in the S1 system, which can be attributed to the formation of blisters and modification of the finishing coating, as seen in the previous sections.

When comparing the anti-graffiti products, no relevant C_c variation was observed in the specimens with the AG2, with exception of system S4. In fact, results showed that the capillary absorption coefficient of the system finished with the silicate-based finishing coat was significantly affected with all the anti-graffiti products after artificial aging. This trend can also be attributed to the low chemical affinity (and thus bonding) among the inorganic, silicate coating and the polymeric (based on acrylic or siloxane) anti-graffiti products.

Drying kinetics

When comparing the reference specimens, system S1 (cementitious base coat and acrylic finishing coat) had the lowest drying rates in phase 1 (DR1), whereas the S2 system (lime-based rendering system) showed the highest DR1 (Fig. 10) and thus most effective drying capacity. In this first step of drying (the constant drying period), water transport is in the liquid state, and the drying front is at the surface, controlled by the external conditions (Hall and Hoff 2012). A similar trend was observed in the second step of drying (DR2), where drying occurs in the vapor phase, and system S2 presented again the highest value and thus fastest drying (Fig. 11). In fact, the higher porosity of the lime-based coat, when compared to the acrylic or silicate-based coating, favored a faster water evaporation.

After the application of the anti-graffiti products, a decrease in the DR1 and DR2 rates was generally observed, due to the formation of a polymeric film with water-repellent properties. No significant differences were observed after the application of AG1 and AG2 on S1, which previously showed a minimal water absorption ("Water absorption by capillarity" section), whereas product AG3 affected more significantly both the DR1 and DR2. In fact, AG1 is based on polysaccharides with high water vapor permeability, whereas AG3 formed a rather thick and highly hydrophobic coating.

A decrease in the DR1 and DR2 was generally registered with the application of the graffiti paints, mostly

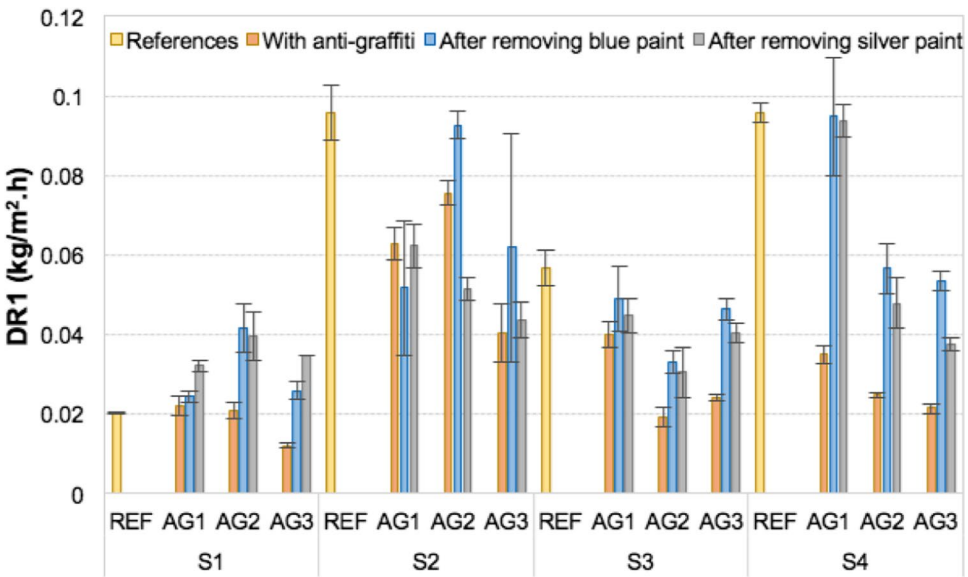

Fig. 10 Drying rate of the first phase (DR1) and relative standard deviation of the reference specimens and after removal of the blue and silver paints

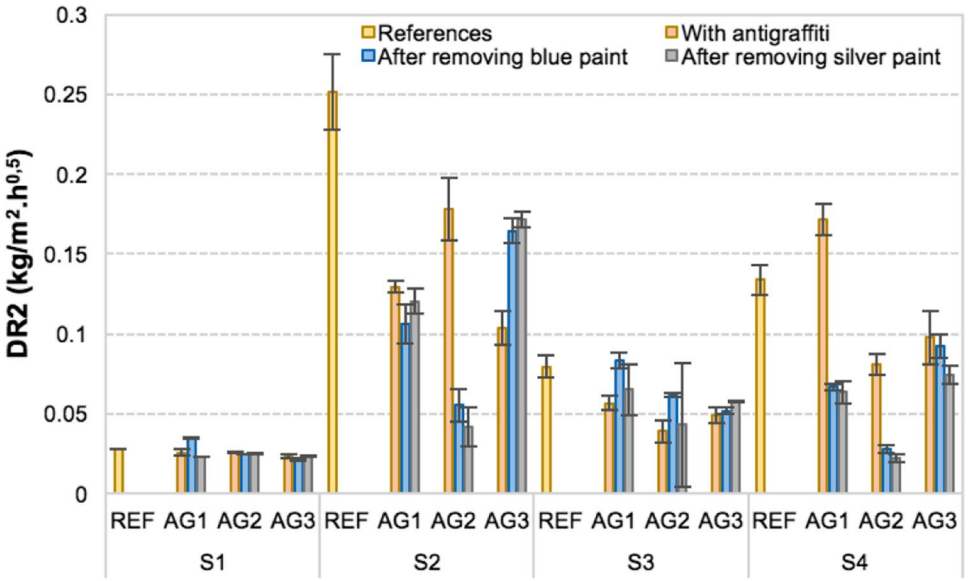

Fig. 11 Drying rate of the second phase (DR2) and relative standard deviation of the reference specimens and after removal of the blue and silver paints

due to the hydrophobic properties and low water vapor permeability of the alkyd or polyethylene-based aerosol spray paint. The highest decreases in DR1 and DR2 rates were noted in the S4.AG2.S (− 79.13%) and S2.AG2.S (− 78.75%) systems, respectively. However, an increase was observed in system S1 (acrylic-based finishing coat) after the application of the silver (S1.AG1.S, S1.AG2.S, and S1.AG3.S) or blue paints (S1.AG2.B).

After the removal of the graffiti paints, it can be noticed a general increase of the DR1 in relation to the results obtained after the application of the graffiti paints (Fig. 10), with values closer to those of the reference specimens. In the case of the system S1, a DR1 increase was observed for the three anti-graffiti products and for both paints (blue and silver), if compared to the values of the initial references, whereas specimens S2, S3, and S4 presented lower values after graffiti removal. In fact, the highest increase of DR1 after removal was observed for specimen S1.AG2.B (+ 104.57%), whereas the highest decrease with specimen S4.AG3.S (− 60.79%), if compared to the reference specimens. Thus, graffiti removal can mostly speed up the water drying in the liquid state of the ETICS with anti-graffiti products, however, with values closer to the reference specimens.

After graffiti removal, the DR2 is lower than that of the pristine specimens (Fig. 11) in the systems S2 and S4, with the highest decrease in specimen S2.AG2.S (− 83.50%). Conversely, systems S1 and S3 showed reduced variations, close to the values of the reference system. The latter results can be attributed to the reduced water absorption of these acrylic-finished systems ("Water absorption by capillarity" section), due to their lower porosity, if compared to the lime-finished system S4.

Although the drying properties of system S1 were not significantly affected by the application of anti-graffiti products and graffiti paints, the systems finished with an acrylic coating (S1 and S3) showed a remarkable increase of both DR1 and DR2 after artificial aging, when compared to the unaged systems (Fig. 12). Product AG3 also induced a noticeable delay of the drying kinetics after aging, due to the increased thickness of this coating and reduced water permeability. On other hand, the anti-graffiti product AG2 would be rather compatible with system S3, due to the hybrid (organic–inorganic) nanostructure with higher breathability.

Conversely, the systems finished with an inorganic coating (S2 and S4) showed an opposite trend, with a low variation or generally a reduction of DR1 and DR2. In fact, the porous structure of the lime-based finishing render of S4 and of the silicate-based topcoat of S9 were possibly affected, with the formation of wider pores which might speed up also the drying kinetics.

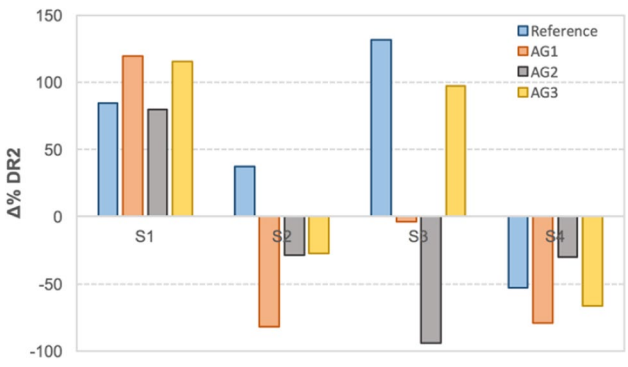

Fig. 12 Variation of the drying rate in the phase of water vapor transport (DR2) among pristine specimens and those after artificial aging

Discussion

Cleaning performance

Results showed that a satisfactory graffiti removal, with a compromise among material conservation and graffiti cleaning, was obtained especially in the case of the systems with an acrylic-finishing coat and EPS as thermal insulation layer (S1 and S3) (Feltes et al. 2023). Nevertheless, the low-invasive method, based on application of anti-graffiti products and on the combination of manual mechanical brushing and low-pressure water vapor jet, still induced a smoothing effect on the cleaned surfaces, with a slight reduction of the surface roughness, possibly affecting the pore size distribution of the finishing coat (Parracha et al. 2021a).

Semi-permanent (AG2) or permanent anti-graffiti products (AG3) showed the most efficient graffiti removal, by modifying the distribution and hindering the adherence of the graffiti paint (Lettieri et al. 2019), especially when applied on ETICS with acrylic-based finishing coats (S1 and S3) ($\Delta E^*_{ab} < 5$). However, the hydrophobicity and/or oleophobicity of these products not always guaranteed optimal results (Lettieri et al. 2019), as in the case of the system with a lime-based rendering system (S2). Furthermore, the polymeric-based anti-graffiti products were less physical–chemical compatible with the silicate-based finishing (S4), leading to a heterogeneous distribution of the anti-graffiti products during their application, as well as to the formation of microcracks (mostly in the case of product AG1).

The application of anti-graffiti products had generally a minimal impact on the surface roughness of the ETICS; however, a yellowish (in the case of the products AG1 and AG3) or whitish (AG2) tones were observed, as well as a relevant gloss increase (in the case of the permanent product AG3). The high roughness of the system S3 might have also hindered the removal of the graffiti.

Previous studies showed that an easier graffiti removal was obtained on smoother surfaces (Rossi et al. 2016) and that anti-graffiti products properly worked when applied on thinner and compact polymeric coatings, rather than thicker and porous films (Masieri and Lettieri 2017). Thus, the application of anti-graffiti products on highly porous substrates should be properly evaluated, since it might form a more heterogeneous, thicker, and less efficient protective layer. Furthermore, the use of anti-graffiti is not recommended on damaged surfaces or on substrates presenting anomalies, e.g., microcracks on the finishing coat, which might lead to the penetration of the product into the substrate and possibly hinder the removal effectiveness of the product.

When comparing the blue and silver graffiti, the easier removal of the blue graffiti can be mainly attributed also to its alkyd nitrocellulose resin binder, which is more flexible and porous if compared to the polyethylene binder of the silver graffiti (Sanmartín and Pozo-Antonio 2020). Furthermore, the removal efficiency depends also on the amount and stability of the pigments (Pellis et al. 2022), and the high content of Al_2O_3 might have hampered the removal of the silver paint. Previous studies with similar paints showed a deposition of alumina particles on surface with silver graffiti after cleaning, whereas the blue paint was identified only within intergranular fissures of rough surfaces (Gomes et al. 2018).

It can be concluded that the cleaning performance of the anti-graffiti action is not only associated to the properties (e.g., composition, roughness) of the treated surface, but strictly depends also on the type of graffiti paint and on the optimization of the cleaning protocol (Lettieri et al. 2019; Sanmartín and Pozo-Antonio 2020).

Effect of graffiti removal on the moisture transport properties

The application of the permanent (AG2) or semi-permanent (AG3) anti-graffiti products sensibly increased the hydrophobicity of the ETICS, as well as slowed down the drying capacity of the surfaces both in the liquid and vapor phase. In fact, system S2 showed a more hydrophilic surface, due to its composition (based on hydrophilic NHL and air lime in the basecoat and finishing coat), if compared to systems S1, S3 (based on a cement-based basecoat and acrylic-based finishing coat), and S4 (with a highly hydrophobic silicate-based finishing coat) (Parracha et al. 2021b).

An increase of the hydrophobicity was observed also after the cleaning of the graffiti paint. The formation of a homogeneous polymeric film with water-repellent properties can induced a reduction of the total porosity of the systems, therefore a limited drying area. Thus, the use of (semi)-permanent anti-graffiti products should be properly evaluated for application on highly humid surfaces (e.g., north-oriented, or with anomalies related to moisture retention within the basecoat or thermal insulation), since the slow drying capacity and breathability of the treated surface might trigger further anomalies (e.g., blistering, stains). The water vapor permeability of the systems with these anti-graffiti products should also be determined, in order to verify if it complies with the requirements of the EAD (EOTA 2019).

Conversely, the sacrificial product AG1, formulated with hydrophilic additives, promoted water absorption by capillarity and slightly delayed the drying process after removal (Rossi et al. 2016). Hence, although this product was almost completely removed after a single graffiti removal action, the application of AG1 may favor water accumulation and thus the bio-susceptibility of the treated surface (Parracha et al. 2022). Additionally, dust accumulation or formation of biological species can lead to enzymatic processes, which might

attack the organic constituents of the finishing, altering the paint binder and surface color (Tator 2015). It is worth mentioning that biocleaning processes have been also tested in the removal of graffiti, using microorganisms capable of specific enzymatic and physiologic responses based on the graffiti composition (Atlas et al. 1991; Sanmartín and Bosch-Roig 2019). Microorganisms can activate specific enzymatic pathways, oxidizing the graffiti components and possibly resulting in color alteration (i.e., graffiti bioremoval) (Bosch-Roig et al. 2021).

Effect of aging on the anti-graffiti products

Another important factor is related to the medium and long-term durability of the anti-graffiti products. In fact, systems showed generally a slight color change (tendency to slight darkening) and a gloss increase after artificial aging (i.e., hygrothermal cycles), in agreement with previous studies (Gomes et al. 2018). Previous research (Parracha et al. 2021b) showed that also UV aging cycles slightly affected the microstructure, gloss, and wettability of the ETICS surface, although the presence of additives with photocatalytical properties (i.e., TiO_2 nanoparticles) provided a self-cleaning capacity to the systems and thus a whitening of the surface. For this reason, it can be argued that the anti-graffiti product AG2, which includes photocatalytical TiO_2 nanoparticles, might have a higher resistance to UV cycles, if compared to product AG1 or AG3. On the other hand, it is worth reporting that, although TiO_2 particles are generally encapsulated in shell materials (e.g., SiO_2, Al_2O_3, or ZrO_2) to prevent the contact between the degradable organics components of the finishing coat and the photoactive TiO_2 surface (thus avoiding discoloration, loss of gloss, or chalking), the long-term durability of the anti-graffiti coating and the photocatalytic effectiveness can be affected by both the poor encapsulation or the weathering of the shell material (Silva et al. 2022).

The system with the hydrophilic lime-based finishing coat (S2) might have favored the leaching of the cork-based insulation layer, with an accumulation of some brownish-pigmented cork particle on the external drying surface. Additionally, the system with a highly rough acrylic-based finishing (S3) showed a yellowish tone on the surface, which is associated to the photo-oxidation of the polymeric matrix (Sanmartín and Pozo-Antonio 2020) and a possible leaching of the mineral wool from the insulation layer. The surface roughness of the systems with lime-based (S2) or silicate-based (S4) finishing was also affected by the aging cycles, due possibly to a partial erosion of the materials (Parracha et al. 2021b).

Although a slight increase of the hydrophilicity of the anti-graffiti products was possibly expectable with aging (Rossi et al. 2017), the hygrothermal cycles induced a significant reduction of the capillary water absorption in the systems, with exception of the system with a low-rough, acrylic-based finishing (S1). This trend can be explained by the leaching of the surface and alteration of the pore size distribution (mainly in the micro and capillary pores) (Parracha et al. 2021b). Conversely, the formation of blisters and alteration of the finishing coating favor the water absorption within the system with acrylic-based finishing and EPS as thermal insulation layer (S1). This latter aspect can be explained by the combined action of water penetration up to the base coat, during the rainy stage of the hygrothermal cycles, and a fast evaporation during the heat stage, which led a consistent vapor pressure from the inner part of the specimens towards the acrylic-based coating (which has a low water vapor permeability) (Parracha et al. 2021a). The previous cleaning action might have played a role in this sense, altering the pore size distribution of the finishing render of system S1. For similar reasons, the drying kinetics was also remarkably affected, with a slowing down of the drying kinetics of systems with lime-based (S2) or silicate-based (S4) finishing and with the permanent anti-graffiti product AG3.

Conclusions

Results showed that the application of the graffiti aerosol paints (blue and silver) affected both the surface properties (color, gloss, roughness) and the moisture transport properties (water absorption and drying kinetic) of the ETICS systems, confirming the need of their removal. In fact, coupled with the alteration of the esthetic aspect of the systems, the formation of highly water-repellent surfaces with low permeability and slow drying kinetics may affect the long-term durability of the systems.

The adoption of a graffiti removal protocol, based on the preventive application of anti-graffiti products and on the combination of manual mechanical brushing and low-pressure water vapor jet, can provide a suitable graffiti cleaning. This innovative protocol is non-toxic and more compatible with the multi-layer composite ETICS systems, when compared to traditional chemical–mechanical removal methods, based on highly acid or basic products or high-pressure water jet.

The application of anti-graffiti products had generally a minimal impact on the surface roughness of the ETICS, however, inducing a yellowish tone (in the case of the sacrificial product AG1 and permanent product AG3) and a relevant gloss increase (in the case of AG3), if compared to the characteristics of the pristine specimens. Additionally, the application of the permanent (AG2) or semi-permanent (AG3) anti-graffiti products sensibly increased the hydrophobicity of the ETICS, as well as slowed down the drying capacity of the surfaces. Conversely, the sacrificial product AG1, also formulated with hydrophilic additives, promoted

water absorption by capillarity and delayed the drying process after removal. Despite its reversibility, the application of AG1 may favor the water accumulation on the treated surface, and thus the durability of the systems.

After graffiti removal, the (semi-)permanent products AG2 and AG3 effectively removed the blue paint and moderately removed silver paint, with a reasonable removal efficiency in the case of systems with acrylic-based finishing (S1 and S3) ($\Delta E^*_{ab} < 5$, i.e., not macroscopically visible hint of graffiti after cleaning). Although the permanent product AG3 guaranteed a more effective anti-graffiti protection, this product cannot be considered completely compatible in the case of inorganic-based specimens (S2 and S4, lime and silicate-based finishing coats), due to its irreversibility and considerable alteration of the optical (gloss and color) ($\Delta E^*_{ab} > 5$) and water transport properties (water absorption 3 to 6 times lower; drying kinetics up to 2 times slower). Finally, the sacrificial product AG1 is not recommended on ETICS, due to its low effectiveness in the removal of the considered aerosol paints ($\Delta E^*_{ab} > 10$).

Based on the artificial aging tests, it was verified that the properties of the anti-graffiti products tend to deteriorate over time, with partial erosion of the material ($\Delta E^*_{ab} > 5$) and alteration of the moisture transport properties (generally lower water absorption and slower drying kinetics). Moreover, these features might possibly affect the effectiveness of the cleaning efficacy over time, considering also that the binder of the spray paints can photo-oxidate with aging, hindering its removal.

Further research is needed to improve the compatibility and effectiveness of anti-graffiti products when applied on inorganic substrates (as in the case of systems S2 and S4, with lime and silicate-based finishing). When dealing with systems with hydrophilic insulating materials (as in the case of system S3, with MW), it should be considered that this material can retain a remarkable amount of water, especially if associated with the formation of microcracks or gaps in the finishing layer. Ultimately, the durability to UV cycles and environmental pollutants should be considered as well, in order to verify the long-term effectiveness of the anti-graffiti products. These data would help to adapt the properties and composition of the ETICS and anti-graffiti products to possible long-term effects also related to climate change.

Acknowledgements Authors acknowledge the Fundação para a Ciência e a Tecnologia (FCT) for funding the project WGB_Shield—_Protection of building facades in the revitalization of cities. Triple resistance to water, graffiti and biocolonization in exterior thermal insulation systems (PTDC/ECI-EGC/30681/2017) and for Ph.D. scholarship (2020.05180.BD—J.L. Parracha), and the support of CERIS Research Centre (UIDB/04625/2020). We would also like to acknowledge the companies CIN, Secil, and Weber Saint-Gobain for supplying the ETICS, as well as the companies NanoPhos and Sika for supplying the anti-graffiti products.

Author contribution All authors contributed to the study conception and design, as well as for the elaboration of the methodology. Material preparation, data collection, formal analysis, and investigation were performed by Bernardo Catita Gil, Giovanni Borsoi, Amélia Dionísio, João Parracha, and Inês Flores-Colen. The first draft of the manuscript was written by Bernardo Catita Gil and Giovanni Borsoi and all authors commented on previous versions of the manuscript. Funding acquisition and resources were managed by Amélia Dionísio, Rosário Veiga, and Inês Flores-Colen. All authors read and approved the final manuscript.

Data availability The authors declare that they will provide any data and materials used in this work, if required.

Declarations

Ethics approval The authors declare that no human participants and/or animals were involved in this work.

Consent to participate and to publish All authors confirmed that they provided a substantial contribution to the conception or design of the work; to the acquisition, analysis, or interpretation of data; to draft the work or revise it. All authors approved to publish the submitted version of the work and agree to be accountable for all aspects of the work in ensuring that questions related to the accuracy or integrity of any part of the work are appropriately investigated and resolved.

Competing interests The authors declare no competing interests.

References

Amaro B, Saraiva D, de Brito J, Flores-Colen I (2014) Statistical survey of the pathology, diagnosis and rehabilitation of ETICS in walls. J Civ Eng Manag 20(4):511–526. https://doi.org/10.3846/13923730.2013.801923

ASTM (2014) ASTM D7089–06: standard practice for determination of the effectiveness of anti-graffiti coating for use on concrete, masonry and natural stone surfaces by pressure washing. ASTM International, West Conshohocken

ASTM (2016) ASTM D2244–16:2016: standard practice for calculation of colour tolerances and colour differences from instrumentally measured colour coordinates. ASTM International, West Conshohocken

ASTM (2018) ASTM D6578/D6578M-13: standard practice for determination of graffiti resistance. ASTM International, West Conshohocken

Atlas MR, Horowitz A, Krichevky M, Bej KA (1991) Response of microbial population to environmental disturbance. Microbiol Ecol 22:249–256. https://doi.org/10.1007/BF02540227

Barreira E, de Freitas VP (2014) External thermal insulation composite systems: critical parameters for surface hygrothermal behaviour. Adv Mater Sci Eng 2014:650752. https://doi.org/10.1155/2014/650752

Boostani H, Modirrousta S (2016) Review of nanocoatings for building application. Procedia Eng 145:1541–1548. https://doi.org/10.1016/j.proeng.2016.04.194

Bosch-Roig P, Pozo-Antonio JS, Sanmartín P (2021) Identification of the best-performing novel microbial strains from naturally-aged graffiti for biocleaning research. Int Biodeterior Biodegrad 159:105206. https://doi.org/10.1016/j.ibiod.2021.105206

Careddua N, Akkoyunb O (2016) An investigation on the efficiency of water-jet technology for graffiti cleaning. J Cult Herit 19:426–434. https://doi.org/10.1016/j.culher.2015.11.009

Carmona-Quiroga PM, Martínez-Ramírez S, Blanco-Varela MT (2008) Fluorinated anti-graffiti coating for natural stone. Mater Construcc 58:233–246. https://doi.org/10.3989/mc.2008.v58.i289-290.76

Carmona-Quiroga PM, Panas I, Svensson JE, Johansson LG, Blanco-Varela MT, Martínez-Ramírez S (2010) Protective performances of two anti-graffiti treatments towards sulfite and sulfate formation in SO_2 polluted model environment. App Surf Sci 257(3):852–856. https://doi.org/10.1016/j.apsusc.2010.07.080

Carvalhão M, Dionísio A (2014) Evaluation of mechanical soft-abrasive blasting and chemical cleaning methods on alkyd-paint graffiti made on calcareous stones. J Cult Herit 16(4):579–590. https://doi.org/10.1016/j.culher.2014.10.004

CEN (2013) EN 16322 - conservation of cultural heritage - test methods - determination of drying properties. European Committee for Standardization (CEN), Brussels, p 2013

CIE (2014) ISO/CIE 11664–6:2014 - colorimetry – part 6: CIEDE2000 colour-difference formula, 2nd edn. CIE, Vienna

Elvira MR, Mazo MA, Tamayo A, Rubio F, Rubio J, Oteo JL (2013) Study and characterization of organically modified silica-zirconia anti-graffiti coatings obtained by sol-gel. J Chem Chem Eng 7:120–131. https://doi.org/10.17265/1934-7375/2013.02.004

EOTA (2019) European Assessment Document - EAD 040083–00–0404: External Thermal Insulation Composite Systems (ETICS) with renderings. EOTA - European Organization for Technical Approvals, Brussels

EU (2018) Directive (EU) 2018/844 of European Parliament and of the Council of 30 May 2018 amending Directive 2010/31/EU on the energy performance of buildings and Directive 2012/27/EU on energy efficiency. Off J Eur Union 156:75-91. Data access 2021-03-15 http://data.europa.eu/eli/dir/2018/844/oj

Feltes J, Borsoi G, Caiado P, Dionísio A, Parracha J, Flores-Colen I (2023) Graffiti removal on external thermal insulation composite systems through chemical-mechanical methods: a feasible protocol?. J Build Eng 105872. https://doi.org/10.1016/j.jobe.2023.105872

Fiorucci MP, Lamas J, Lopez AJ, Rivas T, Ramil A (2011) Laser cleaning of graffiti in Rosa Porrino granite. In: Proceedings of International Conference on Applications of Optics and Photonics, 18-22 July, 80014A, Braga, Portugal. https://doi.org/10.1117/12.892158

García O, Malagab K (2012) Definition of the procedure to determine the suitability and durability of an anti-graffiti product for application on cultural heritage porous materials. J Cult Herit 13:77–82. https://doi.org/10.1016/j.culher.2011.07.004

García O, Rz-Maribona I, Gardei A, Riedl M, Vanhellemont Y, Santarelli ML, Suput JS (2010) Comparative study of the variation of the hydric properties and aspect of natural stone and brick after the application of 4 types of anti-graffiti. Mater Construcc 60(297):69–82. https://doi.org/10.3989/mc.2010.45507

Gaspar P, Hubbard C, McPhail D, Cummings A (2003) A topographical assessment and comparison of conservation cleaning treatments. J Cult Herit 4(1):294–302. https://doi.org/10.1016/S1296-2074(02)01211-6

Germinario G, van der Werf ID, Sabbatini L (2016) Chemical characterisation of spray paints by a multi-analytical (Py/GC–MS, FTIR, μ-Raman) approach. Microchem J 124:929–939. https://doi.org/10.1016/j.microc.2015.04.016

Gomes V, Dionísio A, Pozo-Antonio JS (2017) Conservation strategies against graffiti vandalism on cultural heritage stones: protective coatings and cleaning methods. Prog Org Coat 113:90–109. https://doi.org/10.1016/j.porgcoat.2017.08.010

Gomes V, Dionísio A, Pozo-Antonio JS, Rivas T, Ramil A (2018) Mechanical and laser cleaning of spray graffiti paints on a granite subjected to a SO_2-rich atmosphere. Constr Build Mater 188:621–632. https://doi.org/10.1016/j.conbuildmat.2018.08.130

Graffolution (2016) Awareness and prevention solutions against graffiti vandalism in public areas and transport. SSP (Policy Oriented Research) of the Seventh European Programme of the European Commission (FP7-SEC-2013–1), FP7-SECURITY. Grant agreement ID: 608152. Data access 2021-04-05 https://cordis.europa.eu/project/id/608152/it

Hall C, Hoff WD (2012) Water transport in brick, stone and concrete, 2nd edn. Spon Press, Taylor & Francis Group, New York. https://doi.org/10.1201/b12840

Lettieri M, Masieri M (2014) Surface characterization and effectiveness evaluation of anti-graffiti coatings on highly porous stone materials. App Surf Sci 288:466–477. https://doi.org/10.1016/j.apsusc.2013.10.056

Lettieri M, Masieri M, Pipoli M, Morelli A, Frigione M (2019) Anti-graffiti behavior of oleo/hydrophobic nano-filled coatings applied on natural stone materials. Coatings 9(11):740. https://doi.org/10.3390/coatings9110740

Lubelli B, van Hees RPJ, van de Weert TG (2008) Effect of anti-graffiti coatings on the drying behaviour of building materials. 5th international conference on water repellent treatment of building materials. Aedificatio Publishers, Freiburg, pp 85–94

Malanho S, Veiga MR (2020) Bond strength between layers of ETICS – influence of the characteristics of mortars and insulation materials. J Build Eng 28:101–121. https://doi.org/10.1016/j.jobe.2019.101021

Masieri M, Lettieri M (2017) Influence of the distribution of a spray paint on the efficacy of anti-graffiti coatings on a highly porous, natural stone material. Coatings 7(2):18. https://doi.org/10.3390/coatings7020018

Moura AR, Flores-Colen I, de Brito J (2014) Anti-graffiti products for porous surfaces. An overview. In: Charola AE, Rodrigues JD (eds) Proceedings of *Hydrophobe VII* - 7th international conference on water repellent treatment and protective surface technology for building materials. LNEC – National Laboratory for Civil Engineering, Lisbon, pp 225–233

Moura AR, Flores-Colen I, de Brito J, Dionísio A (2017) Study of the cleaning effectiveness of limestone and lime-based mortar substrates protected with anti-graffiti products. J Cult Herit 24:31–44. https://doi.org/10.1016/j.culher.2016.04.004

Neto E, Magina S, Camões A, Begonha A, Evtuguin DV, Cachim P (2016) Characterization of concrete surface in relation to *graffiti* protection coatings. Constr Build Mater 102(1):435–444. https://doi.org/10.1016/j.conbuildmat.2015.11.012

Parracha JL, Borsoi G, Flores-Colen I, Veiga R, Nunes L, Dionísio A, Gomes MG, Faria P (2021a) Performance parameters of ETICS: correlating water resistance, bio-susceptibility and surface properties. Constr Build Mater 272:121956. https://doi.org/10.1016/j.conbuildmat.2020.121956

Parracha JL, Borsoi G, Veiga R, Flores-Colen I, Nunes L, Garcia AR, Ilharco LM, Dionísio A, Faria P (2021b) Effects of hygrothermal, UV and SO_2 accelerated ageing on the durability of ETICS in urban environments. Build Environ 204:108151. https://doi.org/10.1016/j.buildenv.2021.108151

Parracha JL, Borsoi G, Veiga R, Flores-Colen I, Nunes L, Viegas CA, Moreira LM, Dionísio A, Gomes MG, Faria P (2022) Durability assessment of external thermal insulation composite systems in urban and maritime environments. Sci Total Environ 849:157828. https://doi.org/10.1016/j.scitotenv.2022.157828

Pasker R (2017) The European ETICS market - Do ETICS sufficiently contribute to meet political objectives? 4th European ETICS Forum, EAE – European Association for External Thermal Insulation Composite Systems, 5th October, Warsaw, Poland. https://www.ea-etics.com/publications-events/etics-forum-2017/

Pellis G, Bertasa M, Ricci C, Scarcella A, Croveri P, Poli T, Scalarone D (2022) A multi-analytical approach for precise identification of alkyd spray paints and for a better understanding of their ageing behaviour in graffiti and urban artworks. J Anal Appl Pyrolysis 165:105576. https://doi.org/10.1016/j.jaap.2022.105576

Pozo-Antonio JS, Rivas T, Jacobs RMJ, Viles HA, Carmona-Quiroga PM (2018) Effectiveness of commercial anti-graffiti treatments in

two granites of different texture and mineralogy. Prog Org Coat 116:70–82. https://doi.org/10.1016/j.porgcoat.2017.12.014

Rabea MA, Mohseni M, Mirabedini SM, Tabatabaei HM (2012) Surface analysis and anti-graffiti behavior of a weathered polyurethane-based coating embedded with hydrophobic nano silica. App Surf Sci 258(10):4391–4396. https://doi.org/10.1016/j.apsusc.2011.12.123

Ribeiro T, Dionísio A, Aires-Barros L (2014) Aerosol-paint graffiti: the effects on calcareous stone. Restor Build Monum 15(1):51–66. https://doi.org/10.1515/rbm-2009-6272

Ricci C, Gambino F, Nervo M, Piccirillo A, Scarcella A, De Stefanis A, Pozo-Antonio JS (2020) Anti-graffiti coatings on stones for historical buildings in Turin (NW Italy). Coatings 10(6):582. https://doi.org/10.3390/coatings10060582

Rivas T, Pozo S, Fiorucci MP, López AJ, Ramil A (2012) Nd:YVO4 laser removal of graffiti from granite. Influence of paint and rock properties on cleaning efficacy. Appl Surf Sci 263:563–572. https://doi.org/10.1016/j.apsusc.2012.09.110

Roncon R, Borsoi G, Parracha JL, Flores-Colen I, Veiga R, Nunes L (2012) Impact of water-repellent products on the moisture transport properties and mould susceptibility of external thermal insulation composite systems. Coatings 11(5):554. https://doi.org/10.3390/coatings11050554

Rossi S, Fedel M, Petrolli S, Deflorian F (2016) Behaviour of different removers on permanent anti-graffiti organic coatings. J Build Eng 5:104–113. https://doi.org/10.1016/j.jobe.2015.12.004

Rossi S, Fedel M, Petrolli S, Deflorian F (2017) Characterization of the anti-graffiti properties of powder organic coatings applied in train field. Coatings 7(5):67. https://doi.org/10.3390/coatings7050067

Sanmartín P, Bosch-Roig P (2019) Biocleaning to remove graffiti: a real possibility? Advances towards a complete protocol of action. Coatings 9(2):104. https://doi.org/10.3390/coatings9020104

Sanmartín P, Pozo-Antonio JS (2020) Weathering of graffiti spray paint on building stones exposed to different types of UV radiation. Constr Build Mater 236:117736. https://doi.org/10.1016/j.conbuildmat.2019.117736

Sanmartín P, Cappitelli F, Mitchell R (2014) Current methods of graffiti removal: a review. Constr Build Mater 71:363–374. https://doi.org/10.1016/j.conbuildmat.2014.08.093

Silva AS, Borsoi G, Parracha JL, Flores-Colen I, Veiga R, Faria P, Dionísio A (2022) Evaluating the effectiveness of self-cleaning products applied on external thermal insulation composite systems (ETICS). J Coat Technol Res 19:1437–1448. https://doi.org/10.1007/s11998-022-00617-x

Tator KB (2015) Coating deterioration. In: ASM handbook - volume 5B, Protective organic coatings. ASM International. https://doi.org/10.31399/asm.hb.v05b.9781627081726

Urquhart D (1999) The treatment of graffiti on historic surfaces – advices on graffiti removal procedures, antigraffiti coatings and alternative strategies. Technical Advice Note 18. Technical Conservation Research and Education Division, Historic Scotland

Zhang X, Li H, Harvey JT, Liang X, Xie N, Jia M (2021) Transp Res D: Transp. Environ 101:103101. https://doi.org/10.1016/j.trd.2021.103101